UNIVERSITÀ DEGLI STUDI DI PADOVA

Dipartimento di Fisica e Astronomia "Galileo Galilei"

Corso di Laurea in Fisica

Tesi di Laurea

Hyperfine structure of the hydrogen and evidence for dark matter in spiral galaxies

Relatore

Prof. Francesco D'Eramo

Laureando

Federico Cima

Anno Accademico 2019/2020

Contents

Introduction

Dark matter has a crucial role in our understanding of modern cosmology, since it dominates the mass budget of the universe. The present work is motivated by a personal interest in this topic and it introduces all the basic tools needed to understand how the study of the hydrogen atom has been a turning point in astronomy in the 60s. Indeed, the advent of radio astronomy allowed to collect robust evidences of the existence of dark matter.
In the first chapter, we summarize the standard results on the ideal hydrogen atom. The emphasis is particularly put on the symmetries of the system and how they can justify the high degeneracy of the energy levels. In the second chapter, we systematically introduce all the formalism necessary to take into account the fine structure terms. We present the Lorentz group, its algebra, its spinorial representation and the Dirac equation. Finally we derive the relativistic wave equation for the electron. Using the latter equation, in the third chapter, we first discuss the physical origin of the fine structure terms and why they partially break the degeneracy of the energy levels. Then we compute the energy correction through perturbation theory. Even if we do not take into account the second quantization, we qualitatively present the Lamb shift and in more detail the hyperfine structure. In particular, we show how the famous 21cm line emerges from an hyperfine transition. Finally in the fourth chapter, we review the principal dark matter evidences from observational astronomy. In particular, we mention Zwicky's pioneering work and other more convincing evidences obtained studying the galactic rotational curves. Moreover, we will introduce the most significant dark matter characteristics that are fundamental in order to set up a proper experiment for its detection.

Notation The units are set so that $\hbar = c = 1$ and also $\epsilon_0 = \mu_0 = 1$.
We will use the covariant formalism with the metric signature $\eta_{\mu\nu} = (+, -, -, -)$.
Greek indices take values $\mu = 0, 1, 2, 3$, whereas latin indices take values $i = 1, 2, 3$.
A letter in **boldface** denotes a spatial vector whose components have upper indices.
We define: $\sigma^\mu = (1, \sigma^i)$ and $\bar{\sigma}^\mu = (1, -\sigma^i)$, where σ^i are the Pauli matrices.
We will denote the fine structure constant $\alpha = \frac{e^2}{4\pi\epsilon_0\hbar c}$, where e is the electron charge (defined negative, i.e. $e < 0$).

Chapter 1

The ideal hydrogen atom

1.1 Symmetries of the system

The ideal hydrogen atom consists in a heavy proton, thus essentially motionless, with charge $-e$ and in a nonrelativistic electron with charge e, which orbits around the proton bounded by the electromagnetic field. If we put the proton in the origin of the reference frame, then the potential felt by the electron is

$$V(r) = -\frac{e^2}{4\pi r} = -\frac{\alpha}{r}, \tag{1.1}$$

that is a central potential.
This type of potential has three important symmetries, i.e. transformations under which the Hamiltonian is invariant. Considering the fact that the Hamiltonian is the generator of time translations, then these three symmetries convert into three conservation laws.
First, because of the spherical symmetry of the potential, the electron Hamiltonian H is invariant under rotations. This means that the generator of spatial rotations, i.e. the angular momentum $\boldsymbol{L}$, and also $\boldsymbol{L}^2$ commute with H. Indeed we have:

$$[H, L^i] = 0 \quad \Longrightarrow \quad [H, \boldsymbol{L}^2] = [H, L^i L^i] = [H, L^i]L^i + L^i[H, L^i] = 0. \tag{1.2}$$

Let's denote the Hilbert space of the electron as $\mathcal{H} = L^2(\mathbb{R}^3, d^3x) \simeq L^2(\mathbb{R}_+, r^2dr) \otimes L^2(\mathcal{S}^2, d\Omega)$, where we have exploited the spherical coordinates isomorphism.
In general $\{\boldsymbol{L}^2, L^3\}$ are a complete set of commuting observables (CSCO) for the angular part of $\mathcal{H}$, i.e. $L^2(\mathcal{S}^2, d\Omega)$. It can be shown that $\{H\}$ forms a CSCO for the radial part of $\mathcal{H}$, thus $\{H, \boldsymbol{L}^2, L^3\}$ is a CSCO for the entire $\mathcal{H}$. Thus, $\{H, \boldsymbol{L}^2, L^3\}$ have a common basis of eigenstates $\psi_{nlm_l} = |nlm_l\rangle$, i.e. satisfying

$$H\,|nlm_l\rangle = E(n)\,|nlm_l\rangle, \qquad \boldsymbol{L}^2\,|nlm_l\rangle = l(l+1)\,|nlm_l\rangle, \qquad L^3\,|nlm_l\rangle = m\,|nlm_l\rangle. \tag{1.3}$$

Therefore the quantum numbers n, l, m_l are suitable to describe the system, as they uniquely specify a bound state of the Hamiltonian. In particular:

$$n = 1, 2, \ldots, \qquad l = 0, 1, \ldots, n-1, \qquad m_l = -l, \ldots, l. \tag{1.4}$$

Secondly, since the potential scales as $1/r$ there is a conserved quantity called Laplace-Runge-Lenz vector $\boldsymbol{M}$, defined as in the classical case as

$$M^i = \frac{\epsilon^{ijk} p^j L^k - \epsilon^{ils} L^l p^s}{2m} + V(r)\, r^i, \tag{1.5}$$

where $\boldsymbol{p}$ and m are respectively the momentum operator and the electron mass.
One can verify that this operator has the following properties

$$[H, M^i] = 0, \qquad [L^i, M^j] = i\epsilon^{ijk} M^k, \qquad [M^i, M^j] = -\frac{2i}{m}\epsilon^{ijk} L^k H,$$
$$\boldsymbol{M}^2 = \alpha^2 + \frac{2}{m} H(\boldsymbol{L}^2 + 1), \qquad M^i L^i = 0. \tag{1.6}$$

Finally, the third symmetry of the potential is its invariance under parity transformations. In particular the parity operator P, contrary to $\boldsymbol{M}$, commutes[1] with all $H, \boldsymbol{L}^2$ and L^3, so their eigenstates are also parity eigenstates. Hence the latter must be even or odd,

$$P\,|nlm_l\rangle = (-1)^l\,|nlm_l\rangle. \tag{1.7}$$

1.2 Schröedinger equation and energy degeneration

The Schrödinger equation for the electron in spherical coordinates (r, θ, ϕ) is:

$$-\frac{1}{2m}\left[\frac{1}{r^2}\frac{\partial}{\partial r}\left(r^2\frac{\partial\psi}{\partial r}\right) + \frac{1}{r^2\sin\theta}\frac{\partial}{\partial\theta}\left(\sin\theta\frac{\partial\psi}{\partial\theta}\right) + \frac{1}{r^2\sin^2\theta}\left(\frac{\partial^2\psi}{\partial\phi^2}\right)\right] + V(r)\psi = E\psi. \tag{1.8}$$

As well known, in this case the normalized solutions for bounded states are:

$$\psi_{nlm_l} = \sqrt{\left(\frac{2}{na}\right)^3\frac{(n-l-1)!}{2n(n+l)!}}\,e^{-r/na}\left(\frac{2r}{na}\right)^l\left[L^{2l+1}_{n-l-1}(2r/na)\right]Y_l^{m_l}(\theta,\phi) \tag{1.9}$$

where a is the Bohr radius defined as $a = \frac{1}{m\alpha}$, L^p_q are the associated Laguerre polynomials and $Y_l^{m_l}$ are the spherical harmonics. Besides, the allowed energies are:

$$E(n) = -\left(\frac{1}{2ma^2}\right)\frac{1}{n^2}. \tag{1.10}$$

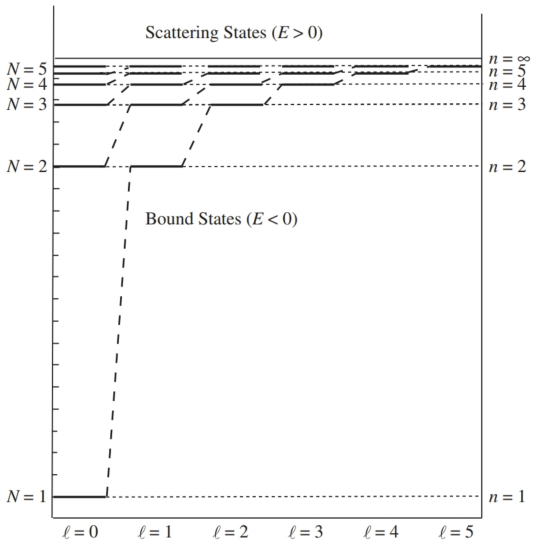

Figure 1.1: Energy levels for ideal hydrogen. One can appreciate the degeneration at fixed principal quantum number n.

Since the energy levels depend only on the principal quantum number n, there is a high degeneration of the states (see Fig.(1.1)). In particular, using Eq.(1.4), the total degeneracy $d(n)$ of

[1] This fact does not contradict the previous assertion that $\{H, \boldsymbol{L}^2, L^3\}$ is a CSCO for $\mathcal{H}$. It simply means that the parity operator can be expressed in terms of these three operators, explicitly $P = (-1)^L$.

each level is:

$$d(n) = \sum_{l=0}^{n-1}(2l+1) = n^2. \tag{1.11}$$

All these degenerations can be explained through the symmetries emphasized in the previous section. The idea is that there is energy degeneration when the Hamiltonian is invariant under a transformation, which on the other hand modifies states. This happens if there are multiple non-commuting symmetry operators, as the impossibility of finding a common basis of eigenstates leads to inevitable degeneracy.
From Eq.(1.7), it is clear that parity does not produce degeneration, in fact P transforms a state into itself up to a sign. Then the degeneration is entirely contained in the other two symmetries. Let's consider rotations. Performing a rotation, it is possible to transform the wave function ψ_{nlm_l} into another one with the same n and l, but different m_l. The explicit relation is obtained using the raising and lowering operators $L_\pm = L^1 \pm iL^2$: $L_\pm|nlm_l\rangle \propto |nl(m_l \pm 1)\rangle$. Through this procedure, for fixed n, it is possible to reach $2l+1$ different eigenstates, but not to jump to different values of l. Thus, rotational symmetry alone justifies only the degeneration of the energy levels with common m, in other terms that Eq.(1.10) does not depend on m_l. As far as rotations the remaining degeneracy is accidental.
An analogue method can be pursued with the Laplace-Runge-Lenz vector. In this case too, it is possible to construct similar raising and lowering operators $M_\pm = M^1 \pm iM^2$. In particular, it is sufficient to note that

$$M_+|nll\rangle \propto |n(l+1)(l+1)\rangle, \tag{1.12}$$

then when M_+ acts on eigenkets with the maximum possible value of m_l, it raises both the indeces l and m_l (unless $l = n-1$). This result is enough to justify the remaining degeneracy. Indeed using these transformations together with rotation, we can get all the possible eigenstates at fixed n. Thus, on the basis of symmetry arguments alone, one can deduce that energy levels must depend only on the principal quantum number n.
We should remark that in this final case the symmetry is not explicit[2]. Since $[H, M^i] = 0$, M^i are simply the generators of such a symmetry, as L^i are the generators of rotations.

[2]To give the idea, the symmetry group of the hydrogen atom is formally $SO(4)$, that is the analog of the Lorentz group, but with a Euclidean metric. Hence this is the group of linear transformations that preserve the quantity $d\gamma^2 = w^2 + x^2 + y^2 + z^2$. The transformations that leave w invariant are the spatial rotations. Instead, the transformations that leave $w^2 + (x^i)^2$ invariant are those with generators M^i (they are the analog of Lorentz boosts).

Chapter 2

Field theory

In order to use the most formal approach in the study of the fine structure, it is important to develop a theory consistent both with quantum mechanics and special relativity. To do so, the first step is to understand how the Lorentz symmetry is implemented in field theory, studying the Lorentz group and its representations. Then it is possible to synthesize these concepts for spin 1/2 fermions into the Dirac equation.

2.1 Lorentz group and Lorentz algebra

Definition 2.1.1. *The Lorentz group O(3, 1) is defined as the group of linear coordinate transformations,*

$$x^\mu \to x'^\mu = \Lambda^\mu{}_\nu \, x^\nu$$

which leave invariant the quantity: $ds^2 = \eta_{\mu\nu} \, x^\mu x^\nu = t^2 - x^2 - y^2 - z^2$.

This definition directly implies that the matrix Λ must satisfy:

$$\eta_{\rho\sigma} = \eta_{\mu\nu} \, \Lambda^\mu{}_\rho \, \Lambda^\nu{}_\sigma. \tag{2.1}$$

Then it is straightforward to see that the Lorentz group consists of four disconnected components, depending on the sign of $det\,\Lambda$ and on the sign of the $\Lambda^0{}_0$ component. The possibilities are $det\,\Lambda = \pm 1$ and $\Lambda^0{}_0 \geq 1 \ \vee \ \Lambda^0{}_0 \leq -1$. In the study of the group one can concentrate only on the component continuously connected with the identity, that is the subgroup of proper[1] ($det\,\Lambda = 1$) and orthochronous ($\Lambda^0{}_0 \geq 1$) Lorentz transformations. The other three components can be obtained from this one through a discrete transformation, such as parity P, time inversion T and space-time inversion PT. For this reason, every time we mention the Lorentz group we will refer only to that component.
Let us consider now an infinitesimal transformation

$$\Lambda^\mu{}_\nu = \delta^\mu_\nu + \omega^\mu{}_\nu, \tag{2.2}$$

therefore Eq.(2.1) gives at the leading order

$$\omega_{\mu\nu} = -\omega_{\nu\mu}. \tag{2.3}$$

Thus, the Lorentz group has six parameters, corresponding to three boosts and three rotations. Having six parameters, the Lorentz group has also six generators. It is convenient to label the generators as $J^{\mu\nu}$, with μ, ν antisymmetric indices. Using the exponential map is thus possible to write a generic element of the group Λ as

$$\Lambda = e^{-\frac{i}{2}\omega_{\mu\nu} J^{\mu\nu}}. \tag{2.4}$$

[1] The subgroup characterized by $det\,\Lambda = 1$ is called proper Lorentz group and it is denoted $SO(3,1)$.

In general, a set of objects ϕ^i, with $i = 1, ..., n$, given an arbitrary n-dimensional representation of the Lorentz group R, transforms under a Lorentz transformation as

$$\phi^i \to \left[e^{-\frac{i}{2}\omega_{\mu\nu}J_R^{\mu\nu}}\right]^i{}_j \phi^j, \tag{2.5}$$

then the relation for an infinitesimal transformation is:

$$\delta\phi^i \to -\frac{i}{2}\omega_{\mu\nu}\left(J_R^{\mu\nu}\right)^i{}_j \phi^j. \tag{2.6}$$

The form of the generators $J_R^{\mu\nu}$ depends on the specific representation. Let us consider the four-vector representation, using Eq.(2.2) and Eq.(2.6), the explicit form for $J^{\mu\nu}$ is given by:

$$(J^{\mu\nu})^\rho{}_\sigma = i(\eta^{\mu\nu}\,\delta^\nu_\sigma - \eta^{\nu\rho}\,\delta^\mu_\sigma). \tag{2.7}$$

Since this representation mixes all four indices, it is irreducible, i.e. it does not admit an invariant subspace. Now it is possible to compute the Lie algebra of $SO(3,1)$:

$$[J^{\mu\nu}, J^{\rho\sigma}] = i(\eta^{\nu\rho}J^{\mu\sigma} - \eta^{\mu\rho}J^{\nu\sigma} - \eta^{\nu\sigma}J^{\mu\rho} + \eta^{\mu\sigma}J^{\nu\rho}). \tag{2.8}$$

It is important to remark that the Lie algebra of a group is independent on the considered representation, so this result is completely general.
The Lie algebra can be conveniently rewritten in terms of two spatial vectors,

$$J^i = \frac{1}{2}\epsilon^{ijk}J^{jk}, \qquad\qquad K^i = J^{i0}. \tag{2.9}$$

Their commutation relations are:

$$[J^i, J^j] = i\epsilon^{ijk}J^k, \qquad [J^i, K^j] = i\epsilon^{ijk}K^k, \qquad [K^i, K^j] = -i\epsilon^{ijk}J^k. \tag{2.10}$$

The first relation is the Lie algebra of $SU(2)$, so $\mathbf{J}$ has the physical interpretation of an angular momentum, i.e. the generator of spatial rotations. Instead $\mathbf{K}$ is the boost generator and physically its conservation is connected with the motion of the CM of the system.
Introducing also other two spatial vectors, $\theta^i = \frac{1}{2}\epsilon^{ijk}\omega^{jk}$ and $\eta^i = \omega^{i0}$, one can verify that a general Lorentz transformation can be written as:

$$\Lambda = \exp\{-i\boldsymbol{\theta}\cdot\mathbf{J} + i\boldsymbol{\eta}\cdot\mathbf{K}\}. \tag{2.11}$$

2.2 Spinorial representations

In quantum mechanics it is crucial to characterize transformations that preserve transition probabilities. If such transformation is the representation of a group, then that is a symmetry group for the system. The other essential point is that the transformation[2] has to be an isomorphism of Hilbert spaces, hence it has to be unitary. It is pretty straightforward to find projective representations, but in general it is non-trivial (or even impossible) to find unitary ones. Representation theory guarantees the following important result:

Theorem 2.2.1 (Bargmann)**.** *Assuming very loose conditions on a given connected group G, there is a bijective function between projective representations of G and unitary representations of its universal covering group $\widetilde{G}$.*

[2]Here we refer to continuous transformations, in fact there exists a more general result, the Wigner theorem, for which the operators that preserve transition probabilities are all and only those obtained through canonical projection on the state space from unitary or anti-unitary projective representations. Since representation have to preserve group structure for continuous symmetries, the only possibility is thus a unitary representation, but for discrete representation there is not such constraint.

Since $\widetilde{SO(3)} = SU(2)$, the physically relevant group for rotations is not $SO(3)$ but $SU(2)$. By the definition of universal covering group, $SU(2)$ and $SO(3)$ are homomorphic, hence they have the same Lie algebra,

$$[J^i, J^j] = i\epsilon^{ijk} J^k, \tag{2.12}$$

so they are equivalent at the level of infinitesimal transformations.
It is well known that $SO(3)$ representations are labeled by an index j taking integer values $0, 1, 2, \dots$. Also $SU(2)$ representations are labeled by an index j, but the latter takes both integer and half-integer values $0, 1/2, 1, \dots$. In both cases, the dimension of the representation is given by $2j + 1$. The representation with $j = 1/2$ is called spinorial representation, and it is the fundamental representation of $SU(2)$ since all representations can be obtained as tensor products of spinors. Spinorial representations have dimension 2 and on them $J^i = \frac{\sigma^i}{2}$, where σ^i are the Pauli matrices. In order to study the angular momentum of a quantum system in a Lorentz invariant framework, it is important to construct a spinorial representation of the Lorentz group. This possibility is more evident using the formulation of the Lorentz algebra presented in Eq.(2.10). In fact, defining

$$\mathbf{J}^{\pm} = \frac{\mathbf{J} \pm i\mathbf{K}}{2}, \tag{2.13}$$

the Lorentz algebra can be expressed also as:

$$[J^{+,i}, J^{+,j}] = i\epsilon^{ijk} J^{+,k}, \qquad [J^{-,i}, J^{-,j}] = i\epsilon^{ijk} J^{-,k}, \qquad [J^{+,i}, J^{-,j}] = 0. \tag{2.14}$$

In this form it is evident that $SO(3,1)$ has the same algebra of $SU(2) \times SU(2)$.
Consequently the representations of the Lorentz algebra can labeled by a pair of indeces (j_-, j_+), that take both integer and half-integer values. The representation dimension will be $(2j_- + 1)(2j_+ + 1)$. Since $\mathbf{J} = \mathbf{J}^+ + \mathbf{J}^-$, using the addition momenta rule of quantum mechanics, the possible spin states are in integer steps in the interval: $|j_+ - j_-| \leq j \leq j_+ + j_-$.
This shows that there are two non-equivalent spinorial representations, denoted $(\mathbf{\frac{1}{2}}, \mathbf{0})$ and $(\mathbf{0}, \mathbf{\frac{1}{2}})$. Overall, we refer to the objects belonging to these representations as Weyl spinors and we denote them

$$\psi_L \in \left(\frac{1}{2}, 0\right), \qquad \psi_R \in \left(0, \frac{1}{2}\right). \tag{2.15}$$

ψ_L and ψ_R are respectively named left-handed Weyl spinor and right-handed Weyl spinor.
The non-equivalence of these representation is evident computing directly the generators and then the transformation relations in both cases, exploting Eqs.(2.13) and (2.11):

$$\psi_L \to \Lambda_L \psi_L = \exp\left\{(-i\boldsymbol{\theta} - \boldsymbol{\eta}) \cdot \frac{\boldsymbol{\sigma}}{2}\right\} \psi_L, \qquad \psi_R \to \Lambda_R \psi_R = \exp\left\{(-i\boldsymbol{\theta} + \boldsymbol{\eta}) \cdot \frac{\boldsymbol{\sigma}}{2}\right\} \psi_R. \tag{2.16}$$

2.3 Dirac equation

Using Weyl spinors, one can define consequently Weyl fields in order to describe spin 1/2 particles. For example, a left-handed Weyl field $\psi_L(x)$ transforms under $x^\mu \to \Lambda^\mu{}_\nu \, x^\nu$ as $\psi_L(x) \to \Lambda_L \psi_L(x)$, with Λ_L given in Eq.(2.16). This is actually not sufficient for our scope. Since our final goal is to study the Hydrogen structure, we want to implement a field theory that is invariant under Lorentz transformations and that preserves parity. In fact the electromagnetic interaction does not experimentally violate parity. Such a theory cannot be developed only through Weyl fields, indeed, under a parity transformation $(t, \boldsymbol{x}) \to (t, -\boldsymbol{x})$, $\boldsymbol{K}$ transforms as a vector $\boldsymbol{K} \to -\boldsymbol{K}$ instead $\boldsymbol{J}$ transforms as a pseudovector $\boldsymbol{J} \to \boldsymbol{J}$. Then from Eq.(2.13) it is evident that $(j_-, j_+) \to (j_+, j_-)$, so a spinorial representation of the Lorentz group is not a representation for a parity transformation, unless $j_- = j_+$. For these reasons, we define a Dirac field (in chiral basis)

$$\Psi = \begin{pmatrix} \psi_L \\ \psi_R \end{pmatrix}. \tag{2.17}$$

The latter has the suitable properties under Lorentz and parity transformations:

$$\Psi \to \begin{pmatrix} \Lambda_L & 0 \\ 0 & \Lambda_R \end{pmatrix} \Psi(x), \qquad \Psi \to \begin{pmatrix} 0 & 1 \\ 1 & 0 \end{pmatrix} \Psi(x') \tag{2.18}$$

where Λ_L and Λ_R are given in Eq.(2.16) and the coordinate change under parity is denoted $x^\mu \to x'^\mu$. This is a reducible representation since $\Psi \in (\frac{\mathbf{1}}{\mathbf{2}}, \mathbf{0}) \oplus (\mathbf{0}, \frac{\mathbf{1}}{\mathbf{2}})$.
Now it is possible to write the Dirac Lagrangian, that is the Lagrangian invariant both under Lorentz and parity transformations, built with both left-handed and right-handed Weyl spinors. The possible Lorentz scalars that can be constructed with the latter are $\psi_R^\dagger \psi_L$ and $\psi_L^\dagger \psi_R$, whereas the possible Lorentz invariants linear in the field derivatives are $\psi_L^\dagger \bar{\sigma}^\mu \partial_\mu \psi_L$ and $\psi_R^\dagger \sigma^\mu \partial_\mu \psi_R$. Then the parity invariance constraint implies:

$$\mathcal{L}_D = i\psi_L^\dagger \bar{\sigma}^\mu \partial_\mu \psi_L + i\psi_R^\dagger \sigma^\mu \partial_\mu \psi_R - m(\psi_R^\dagger \psi_L + \psi_L^\dagger \psi_R), \tag{2.19}$$

where the i factors and the real parameter m are justified retrospectively.
In order to obtain the equation of motion, it is necessary to solve the Euler-Lagrange equations,

$$\frac{\partial \mathcal{L}}{\partial \phi_i} - \partial_\mu \frac{\partial \mathcal{L}}{\partial(\partial_\mu \phi_i)} = 0, \tag{2.20}$$

for $\mathcal{L}_D$, considering ψ_L, ψ_L^*, ψ_R and ψ_R^* independent. Varying[3] with respect to ψ_L^* and ψ_R^* one gets:

$$\bar{\sigma}^\mu i\partial_\mu \psi_L = m\psi_R, \qquad \sigma^\mu i\partial_\mu \psi_R = m\psi_L. \tag{2.21}$$

Applying the operator $\sigma^\mu i\partial_\mu$ to the first equation, and exploiting the second and the identity $\sigma^\mu \bar{\sigma}^\nu + \sigma^\nu \bar{\sigma}^\mu = 2\eta^{\mu\nu}$, we get

$$\left(\Box + m^2\right)\psi_L = 0, \tag{2.22}$$

and an analogous equation[4] holds for ψ_R.
The Eqs.(2.21) can be unified in a single equation in term of a Dirac field

$$(i\gamma^\mu \partial_\mu - m)\Psi = 0, \tag{2.23}$$

where γ^μ depends on the chosen representation. The most convenient in the following is the standard representation, instead of the chiral one defined in the previous section, in which

$$\Psi = \frac{1}{\sqrt{2}} \begin{pmatrix} \psi_R + \psi_L \\ \psi_R - \psi_L \end{pmatrix} = \begin{pmatrix} \phi \\ \chi \end{pmatrix}, \quad \gamma^0 = \begin{pmatrix} 1 & 0 \\ 0 & -1 \end{pmatrix}, \quad \gamma^i = \begin{pmatrix} 0 & \sigma^i \\ -\sigma^i & 0 \end{pmatrix}. \tag{2.24}$$

2.4 Relativistic wave equation

In order to use the Dirac equation to describe the electron in the hydrogen atom, we have to modify Eq.(2.23) to take into account the electromagnetic field. To do so, the idea is to extend the minimal substitution carried out in analytical mechanics, when there is a particle of charge q in an electromagnetic field. In particular, it consists in

$$\boldsymbol{p} \to \boldsymbol{p} + q\boldsymbol{A}, \qquad H(\boldsymbol{p}) \to H(\boldsymbol{p}) + q\varphi, \tag{2.25}$$

where φ and $\boldsymbol{A}$ are respectively the scalar and the vector potentials. After energy and momentum quantization, i.e.

$$H \to i\frac{\partial}{\partial t}, \qquad \boldsymbol{p} \to -i\boldsymbol{\nabla}, \tag{2.26}$$

[3] The variation with respect to ψ_L and ψ_R returns the complex conjugate of the same equations.

[4] From this equation, it is straightforward to understand the physical meaning of m. A solution of $\left(\Box + m^2\right)\varphi = 0$ is a plane wave $\varphi = \varphi_0 e^{-ip\cdot x}$. Substituting this solution into the equation, one obtains $p^\mu p_\mu = m^2$. Thus m is the mass of the particle.

the natural analogue of Eq.(2.25) is

$$i\partial_\mu \to i\partial_\mu + qA_\mu. \tag{2.27}$$

This procedure is called minimal coupling of the Dirac field to the electromagnetic field. It is convenient to define $D_\mu = \partial_\mu + iqA_\mu$. In terms of the latter, the equation of motion of a spin 1/2 charged fermion in an electromagnetic field is:

$$(i\gamma^\mu D_\mu - m)\Psi = 0. \tag{2.28}$$

In the non-relativistic limit, the latter equation reduces to a Shröedinger equation. This is possible after the so called first quantization, i.e. after promoting the classical field to a wave function. In the case of the hydrogen atom, $A_\mu = (A_0, 0)$ with $A_0 = -\frac{e}{4\pi r}$. Then in the standard representation (given in Eq.(2.24)) Eq.(2.28) becomes:

$$(i\partial_0 - V - m)\phi = -i\boldsymbol{\sigma}\cdot\boldsymbol{\nabla}\chi, \tag{2.29}$$

$$(i\partial_0 - V + m)\chi = -i\boldsymbol{\sigma}\cdot\boldsymbol{\nabla}\phi. \tag{2.30}$$

We look for positive energy solutions: $\phi(t,\boldsymbol{x}) = e^{-iEt}\phi(\boldsymbol{x})$ and $\chi(t,\boldsymbol{x}) = e^{-iEt}\chi(\boldsymbol{x})$. Using Eq.(2.26) and defining $\epsilon = E - m$, for the stationary solutions we have

$$(\epsilon - V)\phi = \boldsymbol{\sigma}\cdot\boldsymbol{p}\,\chi, \tag{2.31}$$

$$(2m + \epsilon - V)\chi = \boldsymbol{\sigma}\cdot\boldsymbol{p}\,\phi. \tag{2.32}$$

To take the non-relativistic limit, we have to expand the Dirac equation in powers of $\boldsymbol{p}^2/m^2$, keeping corrections $O(\boldsymbol{p}^2/m^2)$ in both the kinetic energy and the potential. This means that we keep terms up to $O(\boldsymbol{p}^4/m^3)$ and $O(V\boldsymbol{p}^2/m^2)$. From Eq.(2.32)

$$\chi = \frac{1}{2m}\left(1 + \frac{\epsilon - V}{2m}\right)^{-1}\boldsymbol{\sigma}\cdot\boldsymbol{p}\,\phi \simeq \frac{1}{2m}\left(1 - \frac{\epsilon - V}{2m}\right)\boldsymbol{\sigma}\cdot\boldsymbol{p}\,\phi. \tag{2.33}$$

Having been promoted to a wave function, Ψ must be normalized. In order to have a direct analogy with the Schröedinger equation, let us define the wave function in terms of a spinor ϕ_S:

$$\int_V d^3x\,\Psi^\dagger\Psi = \int_V d^3x\,[|\phi|^2 + |\chi|^2] =: \int_V d^3x\,|\phi_S|^2. \tag{2.34}$$

Substituting Eq.(2.33) in the latter and keeping only the first order correction, one gets

$$\int_V d^3x\left[|\phi|^2 + \frac{1}{4m^2}(\boldsymbol{\sigma}\cdot\boldsymbol{\nabla}\phi^*)(\boldsymbol{\sigma}\cdot\boldsymbol{\nabla}\phi)\right] = \int_V d^3x\left[|\phi|^2 - \frac{1}{4m^2}\phi^*(\boldsymbol{\sigma}\cdot\boldsymbol{\nabla})(\boldsymbol{\sigma}\cdot\boldsymbol{\nabla})\phi\right], \tag{2.35}$$

where we have exploited $(\boldsymbol{\sigma}\cdot\boldsymbol{\nabla})(\phi^*(\boldsymbol{\sigma}\cdot\boldsymbol{\nabla}\phi)) = (\boldsymbol{\sigma}\cdot\boldsymbol{\nabla}\phi^*)(\boldsymbol{\sigma}\cdot\boldsymbol{\nabla}\phi) + \phi^*(\boldsymbol{\sigma}\cdot\boldsymbol{\nabla})(\boldsymbol{\sigma}\cdot\boldsymbol{\nabla})\phi$, and the fact that the contribution to the integral of the gradient vanishes in the limit $V \to \infty$. Using the identity $\sigma^i\sigma^j = \delta^{ij} + i\epsilon^{ijk}\sigma^k$, we have also $(\boldsymbol{\sigma}\cdot\boldsymbol{\nabla})(\boldsymbol{\sigma}\cdot\boldsymbol{\nabla}) = (\sigma^i\partial^i)(\sigma^j\partial^j) = \partial^i\partial^i + i\partial^i\partial^j\epsilon^{ijk}\sigma^k = \boldsymbol{\nabla}^2$. Then,

$$\int_V d^3x\,|\phi_S|^2 = \int_V d^3x\left[|\phi|^2 - \frac{1}{4m^2}\phi^*\boldsymbol{\nabla}^2\phi\right] = \int_V d^3x\,\phi^*\left(1 + \frac{\boldsymbol{p}^2}{4m^2}\right)\phi. \tag{2.36}$$

Thus we have

$$\phi_S = \left(1 + \frac{\boldsymbol{p}^2}{8m^2} + O\left(\frac{\boldsymbol{p}^4}{m^4}\right)\right)\phi \quad \Longrightarrow \quad \phi = \left(1 - \frac{\boldsymbol{p}^2}{8m^2} + O\left(\frac{\boldsymbol{p}^4}{m^4}\right)\right)\phi_S. \tag{2.37}$$

In order to obtain a Shröedinger-like equation, we also have to express χ in terms of ϕ_S. Keeping as always only first order corrections

$$\chi \simeq \frac{1}{2m}\left(1 - \frac{\epsilon - V}{2m}\right)\boldsymbol{\sigma}\cdot\boldsymbol{p}\left(1 - \frac{\boldsymbol{p}^2}{8m^2}\right)\phi_S \simeq \frac{1}{2m}\left[\boldsymbol{\sigma}\cdot\boldsymbol{p}\left(1 - \frac{\boldsymbol{p}^2}{8m^2}\right) - \frac{\epsilon - V}{2m}\boldsymbol{\sigma}\cdot\boldsymbol{p}\right]\phi_S. \tag{2.38}$$

Plugging Eqs.(2.37) and (2.38) into Eq.(2.31), and noting that $\boldsymbol{p}$ and V do not commute:

$$\left[\epsilon - \frac{\boldsymbol{p}^2}{2m} - V + \epsilon\frac{\boldsymbol{p}^2}{8m^2} + \frac{\boldsymbol{p}^4}{16m^3} + \frac{V\boldsymbol{p}^2}{8m^2} - \frac{1}{4m^2}(\boldsymbol{\sigma}\cdot\boldsymbol{p})V(\boldsymbol{\sigma}\cdot\boldsymbol{p})\right]\phi_S = 0. \tag{2.39}$$

At the lowest order, we recover, as expected, the Schröedinger equation of the ideal hydrogen atom (Eq.(1.8)), that in compact form reads $\epsilon\phi_S = (\frac{\boldsymbol{p}^2}{2m} + V)\phi_S$.
Now it is necessary to rearrange Eq.(2.39), in order to obtain corrections that have a more evident physical meaning. Firstly, the term $\epsilon\frac{\boldsymbol{p}^2}{8m^2}$ can be rewritten as

$$\epsilon\frac{\boldsymbol{p}^2}{8m^2} = \frac{\boldsymbol{p}^2}{8m^2}\epsilon \simeq \frac{\boldsymbol{p}^2}{8m^2}\left(\frac{\boldsymbol{p}^2}{2m} + V\right). \tag{2.40}$$

The difference between a substitution $\epsilon \to \frac{\boldsymbol{p}^2}{2m} + V$ to the right or to the left of $\frac{\boldsymbol{p}^2}{8m^2}$ is $O(\boldsymbol{p}^6/m^4)$, that is negligible. Eq.(2.39) becomes

$$\epsilon\phi_S = \left[\frac{\boldsymbol{p}^2}{2m} + V - \frac{\boldsymbol{p}^4}{8m^3} + \frac{1}{4m^2}\left((\boldsymbol{\sigma}\cdot\boldsymbol{p})V(\boldsymbol{\sigma}\cdot\boldsymbol{p}) - \frac{1}{2}(\boldsymbol{p}^2V + V\boldsymbol{p}^2)\right)\right]\phi_S. \tag{2.41}$$

Using components, the term involving the potential V can be rewritten as

$$\sigma^i\sigma^j p^i V p^j - \frac{1}{2}(\boldsymbol{p}^2V + V\boldsymbol{p}^2) = p^iVp^i + i\epsilon^{ijk}\sigma^k p^i V p^j - \frac{1}{2}(\boldsymbol{p}^2V + V\boldsymbol{p}^2), \tag{2.42}$$

where we have used again the identity $\sigma^i\sigma^j = \delta^{ij} + i\epsilon^{ijk}\sigma^k$.
Besides, since $[p^i, V] = -i\partial^i V = ieE^i$, with $\boldsymbol{E}$ the electric field, then

$$p^iVp^i = (Vp^i + [p^i, V])p^i = V\boldsymbol{p}^2 + ie\boldsymbol{E}\cdot\boldsymbol{p}. \tag{2.43}$$

Thus Eq.(2.42) can be further developed

$$\begin{aligned}(2.42) &= V\boldsymbol{p}^2 + ie\boldsymbol{E}\cdot\boldsymbol{p} - \frac{1}{2}\boldsymbol{p}^2V + i\epsilon^{ijk}\sigma^k([p^i, V] + Vp^i)p^j \\ &= ie\boldsymbol{E}\cdot\boldsymbol{p} + \frac{1}{2}(V\boldsymbol{p}^2 - \boldsymbol{p}^2V) - e\epsilon^{ijk}E^ip^j\sigma^k \\ &= ie(\boldsymbol{E}\cdot\boldsymbol{p} - \boldsymbol{p}\cdot\boldsymbol{E}) - e\epsilon^{ijk}E^ip^j\sigma^k = -\frac{e}{2}(\boldsymbol{\nabla}\cdot\boldsymbol{E}) - e(\boldsymbol{E}\times\boldsymbol{p})\cdot\boldsymbol{\sigma}.\end{aligned} \tag{2.44}$$

Plugging this result in Eq.(2.41)

$$\epsilon\phi_S = \left[\frac{\boldsymbol{p}^2}{2m} + V - \frac{\boldsymbol{p}^4}{8m^3} - \frac{e}{4m^2}\boldsymbol{\sigma}\cdot(\boldsymbol{E}\times\boldsymbol{p}) - \frac{e}{8m^2}(\boldsymbol{\nabla}\cdot\boldsymbol{E})\right]\phi_S. \tag{2.45}$$

Since the potential is purely radial, then $e\boldsymbol{E} = -\boldsymbol{\nabla}V = -\frac{\boldsymbol{r}}{r}\frac{dV}{dr}$, so

$$-\frac{e}{4m^2}\boldsymbol{\sigma}\cdot(\boldsymbol{E}\times\boldsymbol{p}) = \frac{1}{2m^2}\frac{1}{r}\frac{dV}{dr}\boldsymbol{S}\cdot(\boldsymbol{r}\times\boldsymbol{p}) = \frac{1}{2m^2}\frac{1}{r}\frac{dV}{dr}\boldsymbol{S}\cdot\boldsymbol{L}, \tag{2.46}$$

where we have recognized the spin angular momentum $\boldsymbol{S} = \frac{\boldsymbol{\sigma}}{2}$ and the orbital angular momentum $\boldsymbol{L} = \boldsymbol{r}\times\boldsymbol{p}$. Finally, introducing the explicit relation for the potential $V(r) = -\frac{\alpha}{r}$, the definitive equation for ϕ_S is:

$$\epsilon\phi_S = \left[\frac{\boldsymbol{p}^2}{2m} + V - \frac{\boldsymbol{p}^4}{8m^3} + \frac{\alpha}{2m^2r^3}\boldsymbol{S}\cdot\boldsymbol{L} + \frac{\pi\alpha}{2m^2}\delta^{(3)}(\boldsymbol{x})\right]\phi_S, \tag{2.47}$$

where we have used the well known fact that $\boldsymbol{\nabla}^2\frac{1}{r^2} = -4\pi\delta^{(3)}(\boldsymbol{x})$.
Eq.(2.47) shows explicitly, that in the non-relativistic limit the Dirac equation reduces to a Schröedinger equation for an Hamiltonian $H = H_i + H'$, with H_i the Hamiltonian of the ideal hydrogen atom and H' the perturbation. In particular $H' = H_R + H_{SO} + H_D$, i.e. the perturbation is given by three distinct effects, the relativistic correction, the spin-orbit coupling and the Darwin term. Their physical meaning and the degeneracy breaking they imply are discussed in the following. All the carried out calculations are pretty general, since we have used the fact that the potential is purely radial and its analytic expression only in the final steps.

Chapter 3

Fine and hyperfine splitting

3.1 Degeneracy breaking

Actually, the hydrogen atom has much more structure than as presented in the first chapter, where we have neglected many effects. The more significant are those included in the so-called fine structure. They lead to an energy correction which is a factor α^2 smaller than the Bohr energies in Eq.(1.10). Firstly, the electron is a spin 1/2 fermion, then, besides the orbital angular momentum $\boldsymbol{L}$, one has to take into account the spin angular momentum $\boldsymbol{S}$. Indeed we have considered this fact in the derivation of the relativistic wave equation. Now, let us analyze the three fine structure corrections to the hydrogen Hamiltonian obtained in Eq.(2.47), in order to explain their physical meaning and discuss if and how they break the energy degeneracy of the ideal case. They are

$$H_R = -\frac{\boldsymbol{p}^4}{8m^3}, \qquad H_{SO} = \frac{\alpha}{2m^2 r^3}\boldsymbol{S}\cdot\boldsymbol{L}, \qquad H_D = \frac{\pi\alpha}{2m^2}\delta^{(3)}(\boldsymbol{x}), \tag{3.1}$$

respectively the relativistic correction, the spin-orbit coupling and the Darwin term.
H_R is due to the fact that the electron orbits around the proton with speed $v \simeq \alpha$, thus relativistic corrections have to be taken into account to have more accurate predictions. H_R commutes with $\boldsymbol{L}^2, L^3$ and P, but not with $\boldsymbol{M}^2$ and M^i. Therefore, there is a breaking of the degeneracy in l, since it was justified by the conservation of the Laplace-Runge-Lenz vector.
H_{SO} has mainly a dynamical motivation. In the electron reference frame, the proton is not at rest and a charge in motion generates a nonzero magnetic field. The electron feels this magnetic field that interacts with its magnetic dipole moment $\boldsymbol{\mu}$. This interaction has strong consequences in the symmetry of the system. Indeed H_{SO} commutes only with $\boldsymbol{L}^2$ and P, but not with $L^i, \boldsymbol{M}^2$ and M^i. Then, also the invariance under spatial rotation in broken. So, in order to apply the degenerate perturbation theory, one needs to find a new basis in which the perturbations are diagonal. On the other hand, a new symmetry emerges: the invariance under $SU(2)$ rotations. Indeed, $\boldsymbol{J}^2 = (\boldsymbol{L}+\boldsymbol{S})^2$ and J^3 commute with H_{SO} and, in general, with each contribution to the total Hamiltonian. In particular, n, j, l, s, m_j are suitable quantum numbers for the problem. Since for a fermion $s = 1/2$ is fixed and m_j does not appear explicitly in calculations, we will denote this basis as $|njl\rangle$. The $SU(2)$ rotational symmetry, through the same arguments used in the $SO(3)$ case, implies a complete degeneracy in m_j.
Finally, since a particle cannot be localized more precisely than the Heisenberg uncertainty principle predicts, then the electron feels the proton potential averaged over a certain region. This effect is contained in H_D. Being proportional to a Dirac delta, the first order correction of H_D is nonzero only if the wave-function is nonzero at the origin, that is only if $l = 0$. Also H_D commutes with P, so it is the only symmetry of the ideal case that is preserved.
The cumulative effects of these corrections lead to energy levels dependent on n and j. Thus, besides the degeneracy in m_j, there is a more hidden one. Indeed, states with fixed n and j,

but different l, are still degenerate. This suggests the presence of another not evident conserved quantity, which generates a symmetry transformation for the system, as $\boldsymbol{M}$ in the ideal case.

3.2 Fine structure corrections

In this section, we will compute explicitly the first order corrections to the energy levels of the hydrogen atom using the perturbation theory. The unperturbed eigenkets are denoted $|njl\rangle$.

3.2.1 Relativistic correction H_R

In this case, we have to compute $\langle njl|-\frac{\boldsymbol{p}^4}{8m}|njl\rangle$. The Schröedinger equation of the unperturbed system reads $(\frac{\boldsymbol{p}^2}{2m}+V)|njl\rangle = E(n)|njl\rangle$. Then using Eqs.(1.10) and (1.1):

$$\frac{\boldsymbol{p}^2}{2m}|njl\rangle = \left(-\frac{m\alpha^2}{2n^2}+\frac{\alpha}{r}\right)|njl\rangle. \tag{3.2}$$

This observation allows to simplify the calculation:

$$\langle njl|\frac{\boldsymbol{p}^4}{8m}|njl\rangle = \frac{1}{2m}\langle njl|\left(-\frac{m\alpha^2}{2n^2}+\frac{\alpha}{r}\right)^2|njl\rangle = \frac{m\alpha^4}{8n^4}+\frac{\alpha^2}{2m}\langle njl|\frac{1}{r^2}|njl\rangle+\frac{\alpha^3}{4n^2}\langle njl|\frac{1}{r}|njl\rangle. \tag{3.3}$$

At this step, the quickest way to obtain the expected values of $1/r$ and $1/r^2$ is exploiting a rather simple but extremely useful result, the Feynman-Hellman theorem.

Theorem 3.2.1 (Feynman-Hellman)**.** *Consider a quantum system with Hamiltonian $H(\lambda)$, where λ is a generic parameter. Let $E_n(\lambda)$ and $\psi_n(\lambda)$ be respectively the eigenvalues and eigenfunctions of $H(\lambda)$. Then, assuming that the ψ_n form a basis in which $H(\lambda)$ is diagonal,*

$$\frac{\partial E_n}{\partial \lambda} = \langle\psi_n|\frac{\partial H}{\partial\lambda}|\psi_n\rangle.$$

Proof. Let $H(\lambda_0)$ be an unperturbed Hamiltonian. If we consider an infinitesimal perturbing Hamiltonian H' then, $H' = H(\lambda_0+d\lambda)-H(\lambda_0) = \frac{\partial H}{\partial\lambda}\big|_{\lambda=\lambda_0}d\lambda$. From perturbation theory, the energy correction is $dE_n = \langle\psi_n|\frac{\partial H}{\partial\lambda}|\psi_n\rangle d\lambda \implies \frac{\partial E_n}{\partial\lambda} = \langle\psi_n|\frac{\partial H}{\partial\lambda}|\psi_n\rangle$. □

Let's apply the latter result to the unperturbed Hamiltonian of the hydrogen atom radial wave function with the Bohr energies (Eq.(1.10)):

$$H_r = \frac{1}{2m}\left(\frac{d^2}{dr^2}+\frac{l(l+1)}{r^2}\right)-\frac{\alpha}{r}, \qquad E_n = -\frac{m\alpha^2}{2(N+l)^2}, \tag{3.4}$$

where the energy levels are rewritten in the most convenient way for subsequent calculations and N is a fixed integer number (for which of course $n = N+l$).
Setting $\lambda = \alpha$, we get:

$$\frac{\partial E_n}{\partial\alpha} = \langle njl|\frac{\partial H_r}{\partial\alpha}|njl\rangle \quad\implies\quad \langle njl|\frac{1}{r}|njl\rangle = \frac{m\alpha}{n^2}. \tag{3.5}$$

Setting $\lambda = l$, we obtain:

$$\frac{\partial E_n}{\partial l} = \langle njl|\frac{\partial H_r}{\partial l}|njl\rangle \quad\implies\quad \langle njl|\frac{1}{r^2}|njl\rangle = -\frac{m^2\alpha^2}{n^3(l+\frac{1}{2})}. \tag{3.6}$$

Plugging Eqs.(3.5) and (3.6) in Eq.(3.3) and taking into account an extra minus sign, the relativistic correction finally is

$$\Delta E_R = \frac{m\alpha^4}{2}\left(-\frac{3}{4n^2}+\frac{1}{n^3(l+\frac{1}{2})}\right). \tag{3.7}$$

As explained in Sec.(3.1), the relativistic contribution breaks only the degeneracy in l.

3.2.2 Spin-orbit coupling H_{SO}

In this case, the expected value to be computed is $\langle njl|\frac{\alpha}{2m^2r^3}\boldsymbol{S}\cdot\boldsymbol{L}|njl\rangle$. It is convenient to rewrite $\boldsymbol{S}\cdot\boldsymbol{L}$ as $\frac{1}{2}(\boldsymbol{J}^2-\boldsymbol{L}^2-\boldsymbol{S}^2)$. Then,

$$\frac{\alpha}{4m^2}\langle njl|\frac{(\boldsymbol{J}^2-\boldsymbol{L}^2-\boldsymbol{S}^2)}{r^3}|njl\rangle=\frac{\alpha[j(j+1)-l(l+1)-\frac{3}{4}]}{4m^2}\langle njl|\frac{1}{r^3}|njl\rangle. \tag{3.8}$$

In order to evaluate the expectation of $1/r^3$, one can use the Kramers' relation:

$$\frac{s+1}{n^2}\langle r^s\rangle-\frac{(2s+1)}{m\alpha}\langle r^{s-1}\rangle+\frac{s}{4m^2\alpha^2}[(2l+1)^2-s^2]\langle r^{s-2}\rangle=0, \tag{3.9}$$

where s is an integer and in the expected values the basis kets are implicit.
Setting $s=-1$ and exploiting Eq.(3.6),

$$\frac{1}{m\alpha}\langle njl|\frac{1}{r^2}|njl\rangle-\frac{l(l+1)}{m^2\alpha^2}\langle njl|\frac{1}{r^3}|njl\rangle=0 \quad\Longrightarrow\quad \langle njl|\frac{1}{r^3}|njl\rangle=\frac{m^3\alpha^3}{n^3l(l+\frac{1}{2})(l+1)}. \tag{3.10}$$

The fact that the previous equation is not defined for $l=0$ is not a problem. Indeed from Eq.(3.8) it is evident that in that case $\langle njl|\boldsymbol{S}\cdot\boldsymbol{L}|njl\rangle=0$. Thus, plugging Eq.(3.10) in Eq.(3.8), the correction due to the spin-orbit coupling is:

$$\Delta E_{SO}=(1-\delta_{l,0})\frac{m\alpha^4}{4n^3l(l+\frac{1}{2})(l+1)}\Big[j(j+1)-l(l+1)-\frac{3}{4}\Big], \tag{3.11}$$

where $\delta_{l,0}$ is a Kronecker delta.

3.2.3 Darwin term H_D

We have to compute $\langle njl|\frac{\pi\alpha}{2m^2}\delta^{(3)}(\boldsymbol{x})|njl\rangle$. In this case it is possible to go through the integral, since it involves a Dirac delta,

$$\langle njl|\frac{\pi\alpha}{2m^2}\delta^{(3)}(\boldsymbol{x})|njl\rangle=\frac{\pi\alpha}{2m^2}\int d^3x|\psi_{njl}(\boldsymbol{x})|^2\delta^{(3)}(\boldsymbol{x})=\frac{\pi\alpha}{2m^2}|\psi_{njl}(\boldsymbol{0})|^2. \tag{3.12}$$

The states that are nonzero at the origin are all and only those characterized by $l=0$. Then using Eq.(1.9), one gets:

$$|\psi_{njl}(\boldsymbol{0})|^2=\frac{m^3\alpha^3}{\pi n^3}\delta_{l,0}. \tag{3.13}$$

These results imply that the Darwin term correction is:

$$\Delta E_D=\frac{m\alpha^4}{2n^3}\delta_{l,0}. \tag{3.14}$$

3.2.4 Overall fine correction

Adding up all the computed corrections (Eqs.(3.7), (3.11) and (3.14)), we obtain the total fine structure correction ΔE_{FS}:

$$\Delta E_{FS}=-\frac{m\alpha^4}{2n^3}\left[\frac{1}{j+\frac{1}{2}}-\frac{3}{4n}\right]. \tag{3.15}$$

It is remarkable that there is no separate dependence on l. The spin-orbit coupling and the Darwin term together produce a shift, which is smooth in l.
Fig.(3.1) can be compared with Fig.(1.1), we see that all the states are negatively shifted and as anticipated there remains some degeneracy.
Since the electron has a spin $s=1/2$, then using the angular momenta addition rule $|l-\frac{1}{2}|\leq j\leq$

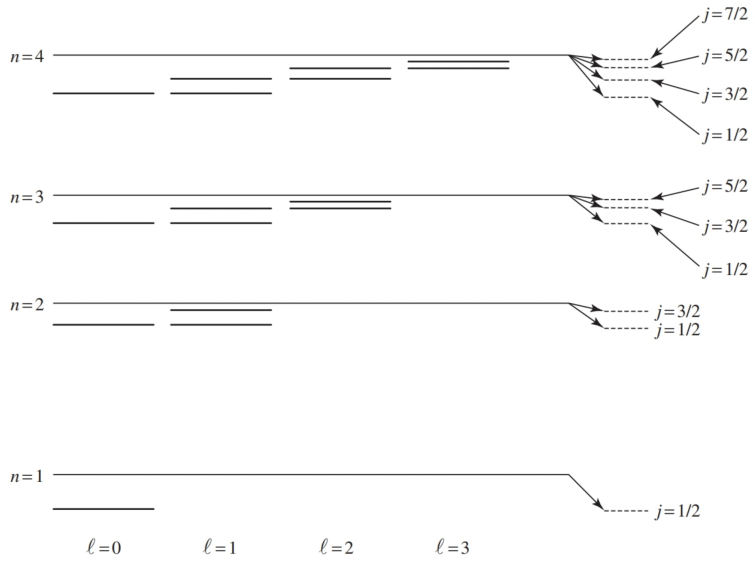

Figure 3.1: Fine structure energy levels for hydrogen. One can appreciate the presence of much less degeneracy at fixed principal quantum number n.

$l + \frac{1}{2}$. Except for the case of maximal value of j, there is the possibility to choose two different values for l that return the same j at fixed n. For this reason, Fig.(3.1) exhibits that pattern. Let us point out that it would not be physically relevant to compute further order corrections. Indeed, starting from the second order of perturbation, the quantum nature of the electromagnetic field and the presence of the proton spin are significant. Taking into account these effects, even more structure emerges: the Lamb shift and the hyperfine structure. These effects are three orders of magnitude smaller than fine splitting. The detailed study of these effects needs more advanced tools than those presented in this work, for this reason in the following section we will present only the results, that are crucial for astronomical applications.

3.3 Hyperfine splitting

3.3.1 Lamb shift

The Lamb shift is purely due to the quantum nature of the electromagnetic field, then the proper framework in which it is justified is QED. Just qualitatively, the physical origin of this effect has three contributions. First, the spontaneous pair production in the vicinity of the nucleus, that produces a partial screening of the nuclear charge. Secondly, the interaction between the electron and the vacuum fluctuations and finally the quantum modification of the magnetic dipole moment. Precise computations lead to:

$$\Delta E_{Lamb} = \begin{cases} \dfrac{\alpha^5 m}{4n^3} k(n,0) & for\ l = 0 \\ \dfrac{\alpha^5 m}{4n^3}\left[k(n,l) \pm \dfrac{1}{\pi(j+\frac{1}{2})(l+\frac{1}{2})}\right] & for\ l \neq 0 \wedge j = l \pm \dfrac{1}{2}. \end{cases} \tag{3.16}$$

$k(n,l)$ is a real number depending on n and l. In general, it picks very small values (less than 0.05), except in the case $l = 0$ in which it is about 10 and the correction is about 10% of the fine structure one. Depending on l, Lamb shift removes the degeneracy between states with the same n and j, but different l.

3.3.2 Hyperfine correction

The hyperfine structure is entirely due to the proton spin. It interacts with both the electron angular momentum and spin, producing the proton spin-orbit coupling and the spin-spin coupling. In order to obtain the hyperfine perturbing Hamiltonian, one can proceed with a classical analogy, even if it is not a formal and systematic approach. The proton spin-orbit coupling H_{PSO}, in analogy with the previously calculated one, is:

$$H_{PSO} = \frac{g_p \alpha^2}{m m_p r^3} \boldsymbol{L} \cdot \boldsymbol{S_p}, \tag{3.17}$$

where g_p[1] is the proton g-factor, m the electron mass, m_p the proton mass and $\boldsymbol{S_p}$ the proton spin. On the other hand, the spin-spin coupling H_{SS} can be evaluated as $H_{SS} = -\boldsymbol{\mu_e} \cdot \boldsymbol{B_p}$, where $\boldsymbol{B_p}$ is the magnetic field due to the proton's magnetic dipole moment and $\boldsymbol{\mu_e}$ is the electron's magnetic dipole moment. From classical electrodynamics[2] we have:

$$\boldsymbol{\mu_p} = \frac{g_p e}{2m_p} \boldsymbol{S_p}, \qquad \boldsymbol{\mu_p} = -\frac{e}{m} \boldsymbol{S_e}, \qquad \boldsymbol{B_p} = \frac{3(\boldsymbol{\mu_p} \cdot \hat{r})\hat{r} - \boldsymbol{\mu_p}}{4\pi r^3} + \frac{2}{3} \boldsymbol{\mu_p} \delta^{(3)}(\boldsymbol{x}). \tag{3.18}$$

Plugging these equations in the relation for H_{SS}, we get:

$$H_{SS} = \frac{g_p \alpha}{2 m m_p r^3} [3(\boldsymbol{S_p} \cdot \hat{r})(\boldsymbol{S_e} \cdot \hat{r}) - \boldsymbol{S_p} \cdot \boldsymbol{S_e}] + \frac{g_p e^2}{3 m m_p} \boldsymbol{S_p} \cdot \boldsymbol{S_e} \delta^{(3)}(\boldsymbol{x}). \tag{3.19}$$

Overall the hyperfine perturbing Hamiltonian is $H_{HS} = H_{PSO} + H_{SS}$. Using perturbation theory, it is possible to compute explicitly the energy correction ΔE_{HS} obtaining,

$$\Delta E_{HS} = \left(\frac{m}{m_p}\right) \frac{\alpha^4 m g_p}{2n^3} \frac{\pm 1}{(f + \frac{1}{2})(l + \frac{1}{2})} \qquad for\ f = j \pm \frac{1}{2}, \tag{3.20}$$

where we have denoted the quantum number of the total angular momentum of the system as f. Thus, from Eq.(3.20), it is clear that the hyperfine correction splits each energy level into a singlet and a triplet.

3.3.3 21cm line

The study of the hydrogen hyperfine structure has been extremely important, particularly for its implications in astrophysics. The transition between the fundamental state of singlet and the one of triplet produce a photon in the radiowave spectrum, with a wavelenght of nearly $21cm$. This radiation penetrates interstellar clouds for very large distances and had a key role in the discovery of dark matter, as we will discuss in the next chapter.
Let's analyze in greater detail the transition

$$1S_{1/2,triplet} \longrightarrow 1S_{1/2,singlet}.$$

Since we are only interested in the energy of the emitted photon, we can neglect the Lamb shift that does not affect the energy difference between the two states. Thus, the splitting is due only to proton spin-orbit coupling and to the spin-spin coupling (see Subsec.3.3.2). The photon energy E_γ is simply

$$E_\gamma = \Delta E_{HS,triplet} - \Delta E_{HS,singlet} = \frac{4 g_p \alpha^4 m^2}{3 m_p}. \tag{3.21}$$

Thus the wavelength of the photon is

$$\lambda = \frac{2\pi}{E_\gamma} \simeq 21.1cm. \tag{3.22}$$

[1] In the previous derivation of the spin-orbit coupling we have not specified explicitly g_e, i.e. the electron g-factor, indeed it is implicitly predicted in the Dirac equation that $g_e = 2$. For the proton the measured value is $g_p \simeq 5.59$, this is an indication that the proton is a composite particle.

[2] Except for the introduction of the g-factors.

Chapter 4

Dark matter evidences from observational astronomy

As we have just mentioned, the study of hydrogen structure has been crucial in finding consistent dark matter (DM) evidences in the 70s. This chapter aims at reviewing the principal astronomical observations that led to such a discovery and at pointing out the essential properties of DM.

4.1 Pioneering Zwicky's work

Since the nineteenth century the mechanism of inferring a mass distribution from the dynamics, dictated by the gravitational interaction, of a nearby system has been used to discover new astronomical objects. The first who used the latter idea to point out the presence of great amount of non-luminous matter in the universe was Fritz Zwicky. In 1933, he studied the redshift of several galaxy clusters, i.e. systems of gravitationally bounded galaxies, and noticed a large scatter in the apparent velocities of eight galaxies in the Coma Cluster. In particular, he applied the virial theorem in order to estimate the average speed of a galaxy in the cluster. Between the theoretical estimate he obtained and the experimental one there is a gap of an order of magnitude. In his further studies, he calculated the mass-to-light ratio of the cluster too. Also in this case he found a value at least one order of magnitude greater than the typical values.
In order to fix these discrepancies, Zwicky hypothesized the existence of a great amount of DM in the cluster that permitted to maintain the system gravitationally bounded and provided the mass to justify such a large mass-to-light ratio. Nevertheless, at that time, astronomers thought that DM was likely to consist of faint stars and other invisible inter-galactic material, so these observations were not perceived as problematic yet.

4.2 Galactic rotation curves

The rotation curves of spiral galaxies, i.e. the velocity profile of the stars and gas in a galaxy as a function of their distance from the galactic center, were historically the second relevant proof of the presence of a huge amount of non-luminous matter in the universe.
The study of these curves increased in the 50s, when Hendrik C. van de Hulst predicted the existence of a 21 cm hyperfine line of neutral interstellar hydrogen. This radio frequency permitted to map the distribution of interstellar hydrogen, called HI region, that is a component of the interstellar medium that was previously invisible, since these regions do not emit in other observational widows. The advent of radio astronomy was revolutionary because radio waves, compared with other wavelengths, are much less affected by adsorption in the interstellar medium, and propagate to a very large distance. Atomic hydrogen has also two crucial properties, first it is cold, i.e. the ratio of its random kinetic energy and its ordered kinetic energy is much smaller

than one, then its dynamics allow to perform accurate measurements of the gravitational field. Second, the HI region often extends well beyond the optical disk, permitting to obtain data at larger radii.
In the 70s, Kent Ford and Vera Rubin collected very precise optical data for the M31 rotation curve, that were then compared with subsequent radio measurements performed by Ford and Whitehurst. Even if M31 is a spiral galaxy, in order to have a theoretical estimate for the velocity profile at very small and very large radii, it is possible to use Gauss' law as if the galaxy were spherical. In such a case:

$$v(r) = \sqrt{\frac{GM(r)}{r}}\,, \tag{4.1}$$

where $M(r)$ is the radial mass distribution, $v(r)$ is the velocity profile and r is the distance from the galactic centre. The luminous part of M31 has a radius of about $r_l \simeq 5 - 10\,kpc$, meanwhile the data for galactic rotation curves extended up to $24\,kpc$[1]. Thus, the theoretical estimate is:

$$v(r) \propto \begin{cases} r & r \ll r_l \\ r^{-1/2} & r \gg r_l\,. \end{cases} \tag{4.2}$$

Indeed, assuming that all the mass is contained within r_l and that for $r \ll r_l$ the mass has a uniform density, then $M(r) \propto r^3$, so Eq.(4.1) implies $v(r \ll r_l) \propto r$. On the other hand, for $r \gg r_l$, $M(r)$ is a constant, hence $v(r \gg r_l) \propto r^{-1/2}$.
In contrast to this prediction, it was observed, both from photometry and radio observations, an approximately flat rotation curve at large galactocentric distances, i.e. for $r > r_l$.

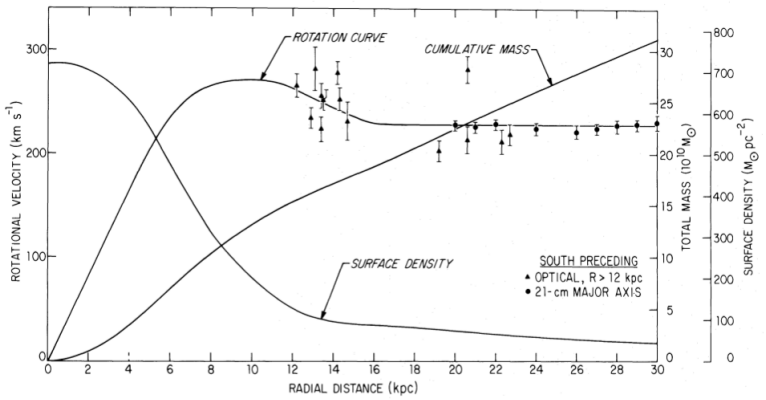

Figure 4.1: M31 rotation curve. The superposition of optical (triangles) and radio (dots) data are showed. The cumulative mass is also reported. As expected from Eq.(4.3), it is approximatively proportional to the radial distance.

By Eq.(4.1), the flattening implies that the mass distribution in the outer regions should be $M(r) \propto r$. So one can infer that the density distribution of DM is:

$$\rho_{DM} \propto \frac{1}{r^2}, \tag{4.3}$$

that is called isothermal mass distribution. It is relevant to notice the implicit assumption that DM has spherical symmetry. Indeed, as we cannot observe it, DM cannot have significant interaction with baryonic matter. Besides, it is likely that DM has at most a very feeble self-interaction, so it is not dissipative and its dynamics is governed primarily by gravity. This argument allows to approximate the DM distribution with a spherical halo around the galaxy.
The Eq.(4.3) is also supported by more recent numerical simulations, in particular we simulate

[1]The above mentioned radio measurements reach $30\,kpc$, while current data go beyond $200\,kpc$.

the process of galaxy formation including a gas of collisionless DM particles. The DM halo, for spiral galaxies, turns out to be spherical as predicted with respect to the previous argument. These simulations also provide more precise relations for the radial density respect to Eq.(4.3). Two common distributions are the Navarro-Frenk-White profile ρ_{DM}^{NFW} and the Einasto one ρ_{DM}^{E},

$$\rho_{DM}^{NFW}(r) = \frac{\rho_n}{(\frac{r}{r_n})(1+\frac{r}{r_n})^2}, \qquad \rho_{DM}^{E} = \rho_e \exp\left[-\frac{2}{\gamma}\left(\left(\frac{r}{r_e}\right)^{\gamma} - 1\right)\right], \tag{4.4}$$

where r_j and ρ_j are parameters depending on the particular galaxy and $\gamma \simeq 0.17$ is a fit parameter of the Einasto profile.

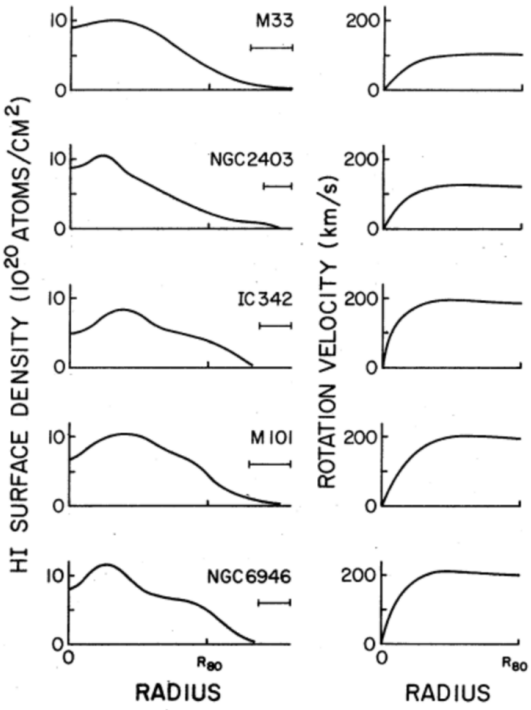

Figure 4.2: Results from the analysis of the five galaxies, M33, NGC2403, IC342, M101 and NGC6946, by Rogstad and Shostak. R_{80} is the radius containing 80% of the HI region.

Right after the work by Rubin and Ford, Rogstad and Shostak performed an analysis of the rotation curves of five galaxies exploiting the HI observations. The idea of their work was to compare the surface density of neutral hydrogen in each galaxy with the corresponding rotation curve. In the first case, they measured the intensity of the 21cm line, whereas in the second case its Doppler shift. The comparison shows that the flattening of the rotation curve is present far beyond the radius at which the HI density is strongly decreasing. The results are presented in Fig.(4.2). In the same years a lot of rotation curves of spiral galaxies were measured and all presented the same trend. These results convinced the scientific community that large amounts of DM were present in the outer regions of galaxies. Nowadays, thanks to the technology development, we have rotation curves up to $200kpc$. In order to build proper detectors for DM particles, the study of the rotation curve of the Milky Way has been particularly intensified, since it is important to quantify the amount of DM present in our galaxy. The task of reconstructing the rotation curve of our galaxy is particularly difficult, since we are inside the system that we want to study. Some recent results (2015) obtained by Iocco et al. are reported in Fig.(4.3). These measurements confirm that the DM halo extends at least tens of kiloparsec more than the galactic disk, indeed in the case of the Milky Way the galactic disk has a radius of approximately $16\,kpc$.

The fact that all the galaxy rotation curves exhibit flat rotation curves at large radii requires fine-tuning between the DM halo and the galactic disk. The unknown mechanism that ensures such a fine-tuning is called conspiracy.

One important point has to be emphasized: it is quite reasonable that at galactic scale the stars, and thus galactic rotation curves, are adequate tracers for DM. In fact, they are in first approximation collisionless and their interactions are governed solely by gravity, as should be for DM as far as we know so far. In order to verify this fact, one can evaluate the mean free time τ for a star in a galaxy, e.g. the Milky Way. It can be obtained as the mean free path λ over the typical velocity of a star v. In particular, the Milky Way has the following characterizing properties:

$$V \simeq 0.2\,Tpc^3\,, \qquad N \simeq 10^{11}\,, \qquad v = 50\,km/s\,, \qquad \langle R_\star \rangle \simeq R_\odot\,, \tag{4.5}$$

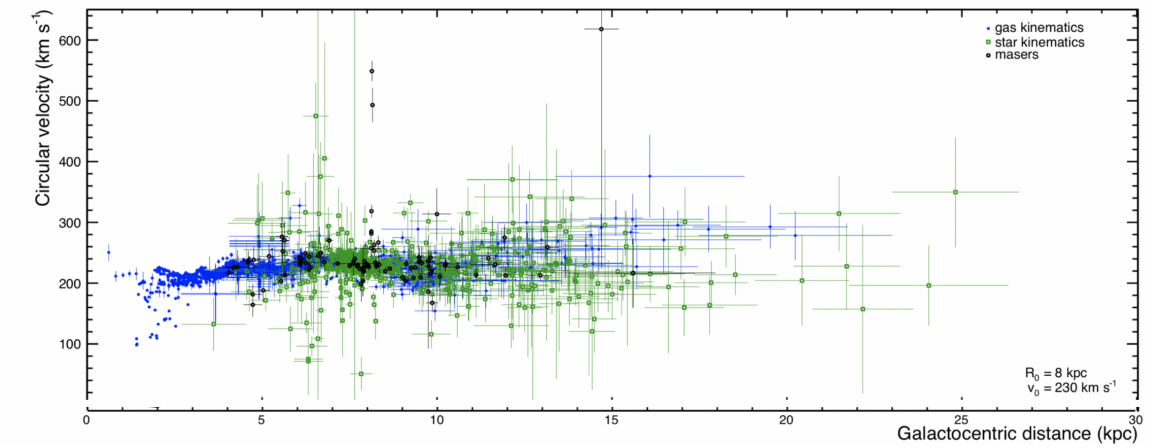

Figure 4.3: Milky Way rotation curve observations. The data obtained from gas kinematics, star kinematics and masers respectively are drawn with different colors. R_0 is the approximate radial position of the Solar system in the Milky Way and v_0 is its circular velocity around the center of the galaxy.

where V indicates its volume, N its number of stars, v the typical star velocity, and $\langle R_\star \rangle$ the average radius of a single star. The mean free path is by definition $\lambda = \frac{N}{V\sigma}$, with σ the cross section of the interaction that in this case is given by $\sigma \simeq \pi \langle R_\star \rangle^2$. Therefore, plugging in the values (4.5), one gets:

$$\tau \simeq \frac{N}{\pi V v \langle R_\star \rangle^2} \simeq 10^{21}\, yr\,. \tag{4.6}$$

This results is far bigger than the lifespan of the Universe, so the not collisionality hypothesis is satisfied.

4.3 From mass distribution to velocity distribution

Using the results presented in the previous section, a natural step forward in characterizing DM is understanding whether it is relativistic or not and its velocity distribution. For the sake of simplicity we will consider Eq.(4.3) as the mass distribution $\rho(r)$ of the DM halo, assumed spherical as before. In order to estimate the mean velocity $\langle v \rangle$ of the DM in the halo, let us consider experimental data from the Milky Way. The estimated mass of its halo is $M_h \simeq 10^{12} M_\odot$, whereas the estimated radius of the halo is $R_h \simeq 100\, kpc$. Applying the virial theorem, the mean velocity can be evaluated as

$$\langle v \rangle = \sqrt{\frac{GM_h}{R_h}} \simeq 200\, km/s. \tag{4.7}$$

Although it is a rough estimate, it tells us that DM is non-relativistic. This result is useful both in studying the velocity distribution of the halo and the particle physics candidates for DM.
Since DM is collisionless and non-relativistic, the one-particle distribution function $f(\boldsymbol{x}, \boldsymbol{v}, t)$ satisfies the collisionless Boltzmann equation

$$\frac{d}{dt} f(\boldsymbol{x}, \boldsymbol{v}, t) = \frac{\partial f}{\partial t} + \boldsymbol{v} \frac{\partial f}{\partial \boldsymbol{x}} + \dot{\boldsymbol{v}} \frac{\partial f}{\partial \boldsymbol{v}} = 0, \tag{4.8}$$

i.e. $f(\boldsymbol{x}, \boldsymbol{v}, t)$ is conserved over time. Let us focus on steady state solutions, i.e. those satisfying $\frac{\partial f}{\partial t} = 0$. In this case, a general theorem holds:

Theorem 4.3.1 (Jeans)**.** *Any steady state solution of the collisionless Boltzmann equation can only be function of integrals of motion of the system.*

Conversely, from the definition of integral of motion, any function of such integrals is a solution to Eq.(4.8). Requiring an additional reasonable condition, i.e. the velocity dispersion tensor of the system $\langle v_i v_j \rangle - \langle v_i \rangle \langle v_j \rangle$ is isotropic, i.e. it is a multiple of the identity, then $f = f(E)$, where E is the total energy of the system. E is certainly a integral of motion, indeed the system is non-dissipative. In the standard thermodynamic limit, all the relevant integrals are exponentials of a dimensionless energy, so we expect that f has this form. For this reason, let us consider the distribution $f(\mathcal{E}) \propto \exp(-\frac{\mathcal{E}}{\sigma^2})$, where $\mathcal{E}$ is the energy per unit mass and σ is the velocity dispersion. Consequently, for the mass distribution we have

$$\rho(r) \propto \int_0^\infty dv\, v^2 f(\mathcal{E}) = \int_0^\infty dv\, v^2 \exp\left(- \frac{v^2/2 + V(r)}{\sigma^2} \right) \propto \exp\left(- \frac{V(r)}{\sigma^2} \right), \tag{4.9}$$

where $V(r)$ is the gravitational potential and we have used the known fact that $\int_0^\infty dx\, x^2 e^{-x^2}$ converges. In order to obtain an explicit relation for $\rho(r)$, we exploit the Poisson equation for the gravitational field $\boldsymbol{\nabla}^2 V(r) = 4\pi G \rho(r)$. Rewriting the Laplace operator in spherical coordinates,

$$\frac{1}{r^2} \frac{d}{dr} \left(r^2 \frac{d \log \rho(r)}{dr} \right) = \frac{4\pi G}{\sigma^2} \rho(r) \qquad \Longrightarrow \qquad \rho(r) = \frac{\sigma^2}{2\pi G r^2} \tag{4.10}$$

Thus, for the velocity distribution we have

$$f(v) \propto \exp\left(- \frac{3v^2}{2\sigma^2} \right), \tag{4.11}$$

where we have used the virial theorem. Then, the initial ansatz on the distribution function was right, a Maxwellian velocity distribution implies an isothermal mass distribution, that is what we wanted to reproduce. Both the mass and velocity distributions obtained are proportional to those of a self-gravitating isothermal gas sphere.

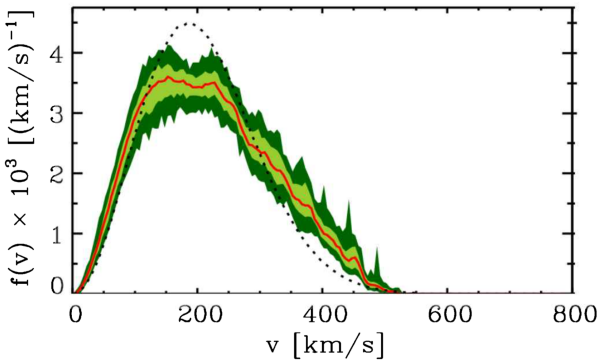

Figure 4.4: Velocity distribution of the Milky Way. In red it is represented the distribution obtained through simulation, in light green its the standard deviation, in dark green the maximum possible range and in dotted black the Maxwell-Boltzmann fit.

Even if the model developed following the initial assumptions explains effectively the qualitative behavior of the system, as we can see from Fig.(4.4), it is important to clarify the limits of those hypothesis. First, Eq.(4.10) implies an infinitely extended and massive DM halo, that is absurd. Indeed, we expect that there exists a radius at which rotation curves are no longer flat. Secondly, the steady state assumption excludes all the collision effects, such as galaxy merging. The impact of these two effects explain, for instance, the presence of clumps and a high-velocity tail in the results of the simulations presented in Fig.(4.4). Primarily for these two reasons, the reference velocity distribution for our galaxy is a Mawellian truncated at the escape velocity of the Milky Way.

Conclusion

The study of hydrogen atom has been important in modern physics for many reasons. Indeed, this is one of the few physically relevant systems that at an ideal level can be solved exactly. The presence of symmetries allows the clear understanding of the degeneration of the energy levels and simplifies calculations. In order to have a systematic way to study this system beyond the ideal case, one has to build a theory that is consistent with both quantum mechanics and special relativity. Such a theory for $1/2$ spin fermions is synthesized in the Dirac equation. In this way it is possible to take into account the fine structure terms and to compute the energy corrections. Considering further effects, i.e. the second quantization and the proton spin couplings, in a systematic way is more involved. The result of the study of these contributions allows to analyze hyperfine transitions of the hydrogen that are fundamental in radio astronomy.
This thesis can be considered an introduction to the fundamental tools that are needed to treat relativistic wave equations, complemented with the calculations for the non-relativistic limit in the case of the hydrogen atom. Finally, we have pointed out the relation between hyperfine structure of hydrogen and the dark matter evidences obtained with rotation curves, giving a review of astronomical dark matter evidences and of its main features such as its mass and velocity distributions. The velocity distribution was found via a pretty general approach that allows to study collisionless and non-relativistic systems.

Bibliography

[1] G. Bertin, *Dynamics of Galaxies*, Cambridge University Press, Cambridge (2014).

[2] G. Bertone and D. Hooper, *A History of Dark Matter*, Rev. Mod. Phys. **90**, 45002 (2018), [arXiv:1811.08797].

[3] F. D'Eramo, *Lecture 1: Dark Matter*, lecture recording, Summer School on Cosmology 2018, Trieste, [ICTP].

[4] D.J. Griffiths, *Introduction to Elementary Particles*, Wiley, New York (1987).

[5] D.J. Griffiths and D.F. Schroeter, *Introduction to Quantum Mechanics*, Cambridge University Press, Cambridge (2018).

[6] F. Iocco, M. Pato and G. Bertone, *Evidence for dark matter in the inner Milky Way*, Nature Physics **11**, 245-248 (2015) [arXiv:1502.03821].

[7] M. Lisanti, *Lectures on Dark Matter Physics*, lecture notes, TASI 2015, Boulder, [arXiv:1603.03797].

[8] M. Maggiore, *A Modern Introduction to Quatum Field Theory*, Oxford University Press, Oxford (2005).

[9] P.A. Marchetti, *Istituzioni di Fisica Teorica*, lecture notes, Padova (2019), [pd.infn].

[10] M.E. Peskin, *Concepts of Elementary Particle Physics*, Oxford University Press, Oxford (2019).

[11] S. Profumo, *An Introduction to Particle Dark Matter*, World Scientific, Singapore (2017).

[12] R. Shankar, *Principles of Quantum Mechanics*, Springer, New York (1994).

[13] J. de Swart, G. Bertone and J.van Dongen, *How Dark Matter Came to Matter*, Nature Astronomy **1**, 0059 (2017), [arXiv:1703.00013].

[14] F. Zwicky, *Die Rotverschiebung von extragalaktischen Nebeln*, Helvetiva Physica Acta **6**, 110-127 (1933) [ADS].